Cell, Vol. 120, 99–110, January 14, 2005, Copyright ©2005 by Elsevier Inc. DOI 10.1016/j.cell.2004.11.032

Coordinated Remodeling of Cellular Metabolism during Iron Deficiency through Targeted mRNA Degradation

Sergi Puig,[1,2] Eric Askeland,[1] and Dennis J. Thiele[1,*]
[1]Department of Pharmacology and Cancer Biology
Sarah W. Stedman Nutrition and Metabolism Center
Duke University Medical Center
Research Drive-LSRC-C351
Durham, North Carolina 27710

Summary

Iron (Fe) is an essential micronutrient for virtually all organisms and serves as a cofactor for a wide variety of vital cellular processes. Although Fe deficiency is the primary nutritional disorder in the world, cellular responses to Fe deprivation are poorly understood. We have discovered a posttranscriptional regulatory process controlled by Fe deficiency, which coordinately drives widespread metabolic reprogramming. We demonstrate that, in response to Fe deficiency, the *Saccharomyces cerevisiae* Cth2 protein specifically downregulates mRNAs encoding proteins that participate in many Fe-dependent processes. mRNA turnover requires the binding of Cth2, an RNA binding protein conserved in plants and mammals, to specific AU-rich elements in the 3′ untranslated region of mRNAs targeted for degradation. These studies elucidate coordinated global metabolic reprogramming in response to Fe deficiency and identify a mechanism for achieving this by targeting specific mRNA molecules for degradation, thereby facilitating the utilization of limited cellular Fe levels.

Introduction

Iron (Fe) is an essential nutrient for virtually all organisms. Fe serves as a cofactor for a wide variety of cellular processes, including oxygen transport, cellular respiration, the tricarboxylic acid (TCA) cycle, lipid metabolism, synthesis of metabolic intermediates, gene regulation, and DNA replication and repair. Despite its abundance in the earth's crust, Fe bioavailability is highly restricted due to its extreme insolubility at physiological pH. Indeed, Fe deficiency is the primary nutritional disorder in the world, estimated to affect over two billion people and resulting in iron deficiency anemia (Baynes and Bothwell, 1990). Alterations in iron homeostasis underlie many human diseases, including Friedreich's ataxia, hereditary hemochromatosis, aceruloplasminemia, Parkinson's disease, aging, microbial pathogenesis, and cancer (Hentze et al., 2004; Nittis and Gitlin, 2002; Roy and Andrews, 2001).

Elegant genetic, biochemical, and physiological studies have elucidated many of the components that function in Fe uptake, efflux, and distribution and their mechanisms of action in both prokaryotic and eukaryotic cells (Escolar et al., 1999; Hentze et al., 2004; Van Ho et al., 2002). Studies with the baker's yeast *Saccharomyces cerevisiae* have demonstrated that, in response to Fe deprivation, cells utilize the Fe-responsive transcription factors Aft1 and Aft2 to induce expression of the so-called iron regulon (Rutherford et al., 2003; Shakoury-Elizeh et al., 2004), which includes proteins involved in Fe reduction at the plasma membrane, uptake, mobilization from intracellular stores, and utilization from heme, among others (Van Ho et al., 2002). Less attention has been dedicated to the characterization of metabolic pathways that are specifically downregulated by Fe depletion. Recent studies have shown that mRNA levels of genes involved in biotin synthesis, glutamate metabolism and heme assembly are downregulated under low Fe conditions (Lesuisse et al., 2003; Shakoury-Elizeh et al., 2004). However, the mechanisms controlling the Fe deprivation-dependent downregulation of these genes, and other global metabolic pathways altered as a consequence of Fe deficiency, have not been elucidated.

In mammals, one response to iron scarcity is posttranscriptionally controlled by the iron-regulatory proteins IRP1 and IRP2. In response to Fe deprivation, IRP1 binds to specific mRNA stem-loop structures known as iron-responsive elements (IREs). IRP1 binding to IREs in the 5′ untranslated region inhibits translation of erythroid aminolevulinic acid synthase, mitochondrial aconitase, the ferroportin Fe efflux pump, and subunits of the Fe storage protein ferritin. IRP1 binding to IREs in the 3′ untranslated region (3′UTR) of the transferrin receptor 1 isoform stabilizes the mRNA, thereby increasing protein levels and enhancing Fe uptake via Fe loaded transferrin (Hentze et al., 2004; Theil, 2000). A posttranscriptional downregulation of Fe-dependent pathways, which depends on small antisense RNAs, has recently been described in bacteria (Masse and Gottesman, 2002; Wilderman et al., 2004).

While several dozen metabolic enzymes require Fe for catalysis in eukaryotic cells, little is known about global reprogramming and regulatory mechanisms governing this process in response to Fe deficiency. We have discovered a mechanism that mediates global posttranscriptional control of multiple components of Fe-dependent pathways to respond in a concerted fashion to Fe deficiency. The Fe-regulated protein Cth2 coordinates this process by binding to and targeting specific mRNA molecules for degradation under Fe deficiency, thereby facilitating the utilization of limited available Fe for normal growth.

Results

Genome-Wide Response of *Saccharomyces cerevisiae* to Iron Deprivation

Although Fe plays a crucial role in a wide array of cellular processes, little is known about how Fe deprivation affects metabolic pathways on a global scale in eukaryotic cells. To investigate the response of *S. cerevisiae* to Fe

*Correspondence: dennis.thiele@duke.edu
[2]Present address: Departament de Bioquimica i Biologia Molecular, Universitat de Valencia, Avenida Dr. Moliner 50, E-46100 Burjassot, Valencia, Spain.

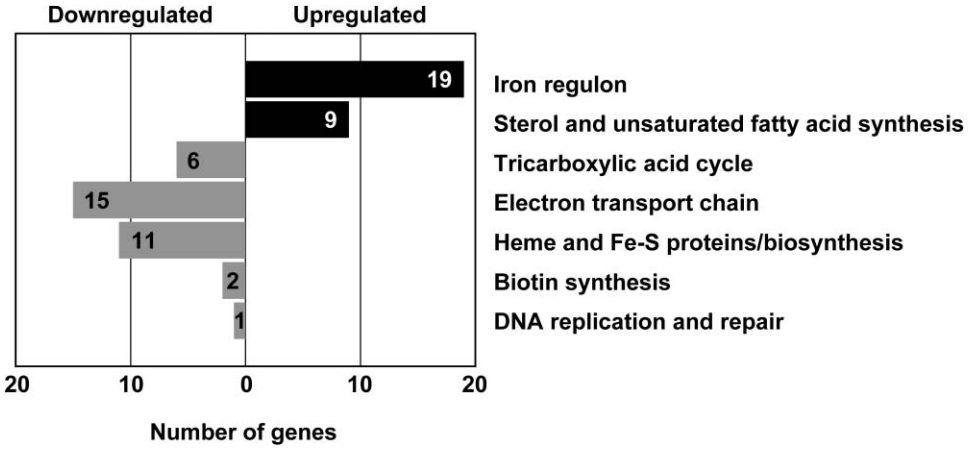

Figure 1. Response of Fe-Dependent Processes to Fe Depletion in Yeast

B4741 wild-type cells were grown in SC containing 300 μM Fe or 100 μM BPS, and RNA was analyzed with DNA microarrays as detailed in Experimental Procedures. Only components of multiple Fe-dependent pathways with a fold change greater than two have been represented. A list of the genes grouped in each functional family is shown in Supplemental Tables S2 and S3.

deprivation, we compared the mRNA expression profile of wild-type cells grown under Fe-replete conditions to cells grown under Fe scarcity achieved by addition of the Fe(II) chelator bathophenantholine disulfonic acid (BPS). We observed that, in addition to changes in other processes (data not shown), key components of multiple Fe-dependent metabolic pathways are significantly altered by Fe availability (Figure 1 and see Supplemental Tables S2 and S3 at http://www.cell.com/cgi/content/full/120/1/99/DC1/). In addition to the induction of the Aft1/2-dependent Fe regulon previously described (Blaiseau et al., 2001; Rutherford et al., 2003; Shakoury-Elizeh et al., 2004; Yamaguchi-Iwai et al., 1996), genes involved in sterol biosynthesis (*ERG* genes) and the fatty acid desaturase *OLE1* are induced under Fe deprivation. In addition, key components of multiple Fe-dependent pathways and proteins including (1) the TCA cycle; (2) the mitochondrial electron transport chain; (3) Fe-S cluster, di-Fe-tyrosyl, and heme-containing proteins; and, (4) as recently described (Lesuisse et al., 2003; Shakoury-Elizeh et al., 2004), *HEM15* encoding ferrochelatase, the last step in heme biosynthesis, and two enzymes involved in biotin synthesis are coordinately downregulated by Fe depletion (Figure 1 and Supplemental Table S3). Taken together, these results demonstrate that mRNA levels of multiple components of Fe-dependent metabolic pathways in *S. cerevisiae* are coordinately regulated in response to Fe deprivation.

The Aft1-Aft2 Target *CTH2* Is Important for Growth under Fe Limitation

Previous DNA microarray experiments strongly suggest that the *CTH2* gene, which encodes a protein related to the mammalian tandem zinc finger (TZF) protein tristetraprolin or TTP (Figure 2A), is transcriptionally induced under Fe limitation (Foury and Talibi, 2001; Rutherford et al., 2003; Shakoury-Elizeh et al., 2004). As shown in Figures 2B and 2C, the steady-state levels of *CTH2* mRNA and a functional FLAG epitope-tagged Cth2 protein under Fe-adequate conditions are very low but dramatically increase in response to Fe deprivation. Furthermore, *CTH2* expression under low Fe conditions is significantly decreased in an *aft1* strain and is undetectable under either condition in the *aft1aft2* double mutant. Mutagenesis of two putative Aft1-Aft2 binding sites (Yamaguchi-Iwai et al., 1996) from the *CTH2* upstream sequence indicates that both sites cooperate in the activation of *CTH2* by Fe starvation, although these experiments do not exclude the participation of other *cis*-regulatory sequences in *CTH2* regulation by Fe (see Supplemental Figure S2 on the *Cell* web site).

Given that *CTH2* mRNA levels are tightly regulated by Fe availability and the Aft1-Aft2 Fe-responsive transcription factors, we assayed growth of *cth2* deletion mutant cells under Fe deprivation conditions. *cth2* cells exhibited a growth defect compared to wild-type cells in the presence of the intracellular Fe-specific chelator ferrozine (Figure 3A). The *cth2* growth defect on ferrozine was reversed by addition of Fe (Figure 3A), demonstrating that the growth defect of *cth2* cells occurs in response to Fe deprivation rather than to ferrozine administration. The yeast genome harbors a gene encoding a protein similar to Cth2, Cth1 (Thompson et al., 1996), whose transcription is independent of Fe levels (Figure 2B). Although *cth1* cells did not display a growth defect under Fe deprivation conditions, cells lacking both *CTH1* and *CTH2* exhibited a more severe growth defect than those lacking only *CTH2* (Figure 3A). Similarly, the *cth1cth2* growth defect in the presence of ferrozine was partially suppressed by *CTH1* and completely recovered by coexpression of both *CTH1* and *CTH2* (Figure 3B). These results demonstrate that *CTH2* is important for growth under Fe deprivation induced by the membrane permeable Fe chelator ferrozine and suggest that Cth1 function in yeast cells may partially overlap with Cth2.

CTH2 Coordinates the Downregulation of Multiple Fe-Dependent Pathways under Fe Deprivation

A prominent feature of Cth2 is the presence of a $Cx_8Cx_5Cx_3H$ tandem zinc finger (TZF) domain near the carboxyl terminus of the protein (Figure 2A and Supplemental Figure S1). This TZF motif is present in a family of

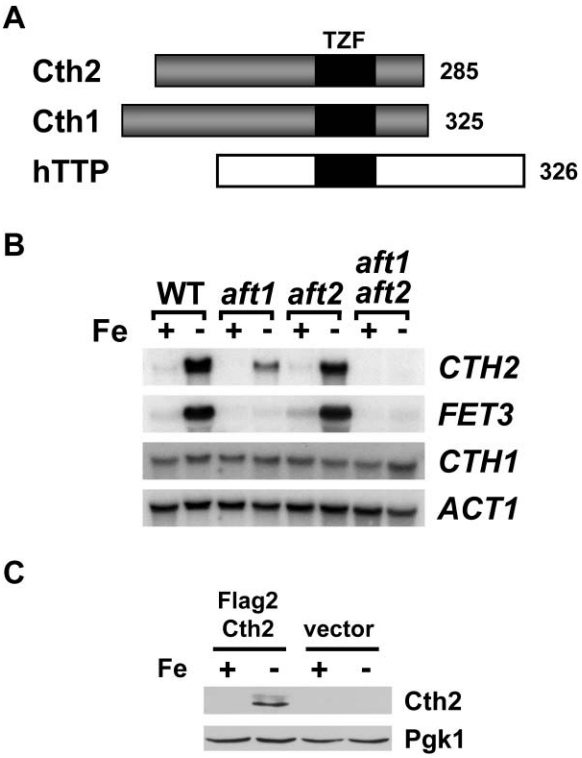

Figure 2. Expression of *CTH2* upon Fe Depletion Is Dependent on Both Aft1 and Aft2 Transcription Factors

(A) Model for the primary structure of *S. cerevisiae* Cth2 and Cth1 and human tristetraprolin (hTTP) protein. TZF, tandem zinc finger.

(B) CM3260 wild-type, *aft1*, *aft2*, and *aft1aft2* cells were grown in SC containing 100 μM Fe (Fe +) or 100 μM BPS (Fe −) and RNA extracted and analyzed by RNA blotting. The Aft1 target *FET3* was used as a control for Fe-regulated expression.

(C) *cth1cth2* cells transformed with pRS416-FLAG2-CTH2 or pRS416 (vector) were grown in SC-Ura containing 300 μM Fe (Fe +) or 100 μM BPS (Fe −) and protein extracted and analyzed by immunoblotting. Phosphoglycerate kinase (Pgk1) was used as a loading control.

RNA binding proteins typified by the mammalian protein tristetraprolin (TTP). TTP mediates the targeted destabilization of tumor necrosis factor α (TNFα), cyclooxygenase-2, interleukin-3, and granulocyte/macrophage colony-stimulating factor (GM-CSF) mRNAs (Blackshear, 2002; Carballo et al., 1998; Sawaoka et al., 2003; Stoecklin et al., 2001). An alignment of yeast Cth1 and Cth2 with human TTP shows that, while Cth1 and Cth2 proteins share 46% identity, hTTP homology to Cth1 and Cth2 is restricted to the TZF domains (Supplemental Figure S1). Despite little homology in the rest of the protein, we hypothesized that Cth2 could be involved in posttranscriptional regulation of specific mRNAs under Fe deprivation. To test this hypothesis, we ascertained the effect of Cth2 on multiple mRNAs we observed in our microarray to be downregulated by Fe deficiency. As shown in Figure 3C, genes encoding proteins involved in the TCA cycle (*SDH4*), heme synthesis (*HEM15*), Fe-S cluster assembly (*ISA1*), vacuolar Fe accumulation (*CCC1*), and Fe-S proteins (*LIP5*) are dramatically downregulated under Fe starvation in a wild-type strain. The mRNA levels of *RNR2*, encoding a subunit of the essential di-Fe-tyrosil-dependent enzyme ribonucleotide reductase, are only modestly decreased by Fe deprivation (Figure 3C). Interestingly, this coordinated mRNA downregulation does not occur in the absence of *CTH2* (Figure 3C, wt versus *cth2* mutant). While mRNA levels in *cth1* cells did not change significantly with respect to wild-type cells, the *cth1cth2* mutant displayed reduced mRNA downregulation, suggesting that Cth1 directly or indirectly influences in this process. These results demonstrate that Cth2 functions in the downregulation of specific mRNAs under conditions of Fe deprivation.

We used DNA microarrays to ascertain which mRNAs exhibit *CTH2*-dependent changes on a genome-wide scale by comparing the gene expression profiles under Fe deficiency of *cth1cth2* cells expressing a plasmid-borne *CTH2* gene or transformed with vector alone. Messenger RNAs corresponding to 84 genes were significantly upregulated in the absence of *CTH2* (Table 1). Interestingly, 54% (45 of 84) of the upregulated genes are involved in obvious Fe-dependent processes, 14% (12 of 84) have other functions, and 32% (27 of 87) are genes of unknown function. Among the 45 Fe-related genes whose expression is increased in *cth2* mutants under low Fe conditions compared to wild-type cells, we find (1) three members of the Fe regulon (*FIT1*, *FIT2*, and *HMX1*); (2) genes encoding key enzymes involved in heme biosynthesis (*HEM15*); (3) two genes encoding proteins involved in Fe-S cluster assembly (*ISA1* and *NFU1*); (4) eight genes encoding enzymes that participate in the TCA cycle including aconitase (*ACO1*), succinate dehydrogenase subunits *SDH2* and *SDH4*, α-ketoglutarate dehydrogenase (*KGD1*), and dihydrolypoyl transsuccinylase (*KGD2*); (5) 15 genes encoding proteins that participate in the electron transfer chain that include four subunits of the cytocrome c oxidase (*COX4*, *COX6*, *COX8*, *COX9*) and six subunits of the ubiquinol cytochrome c reductase complex (*COR1-5* and *RIP1*); (6) eight members of the sterol and unsaturated fatty acid synthesis and metabolism pathways (*ERG* genes and *OLE1*); (7) ribonucleotide-diphosphate reductase subunits (*RNR4*); and (8) genes encoding additional Fe-S cluster-containing proteins (*LIP5*, encoding lipoic acid synthase; *LEU1*, required for leucine biosynthesis; and *RLI1*, related to RNase L inhibitor). Taken together, these results demonstrate that Cth2 functions in the coordinated downregulation of multiple Fe-dependent metabolic pathways, and potentially other as yet uncharacterized pathways, in yeast under conditions of Fe deficiency.

A Conserved RNA Binding Motif Is Required for Cth2-Mediated mRNA Downregulation

Studies with TTP in mammalian systems have demonstrated that the integrity of the zinc finger domains is required for binding and destabilization of specific mRNAs (Blackshear, 2002; Lai et al., 1999, 2003). We tested the role of the CCCH zinc fingers in Cth2-dependent mRNA downregulation by mutagenizing conserved cysteine residues, located in both zinc finger motifs, to arginine. First, cells expressing *CTH2-C190R* or *CTH2-C213R* mutant alleles displayed a growth defect in the presence of the Fe-chelator ferrozine (Figure 3E). Second, Cth2-dependent downregulation of *SDH4*, *HEM15*,

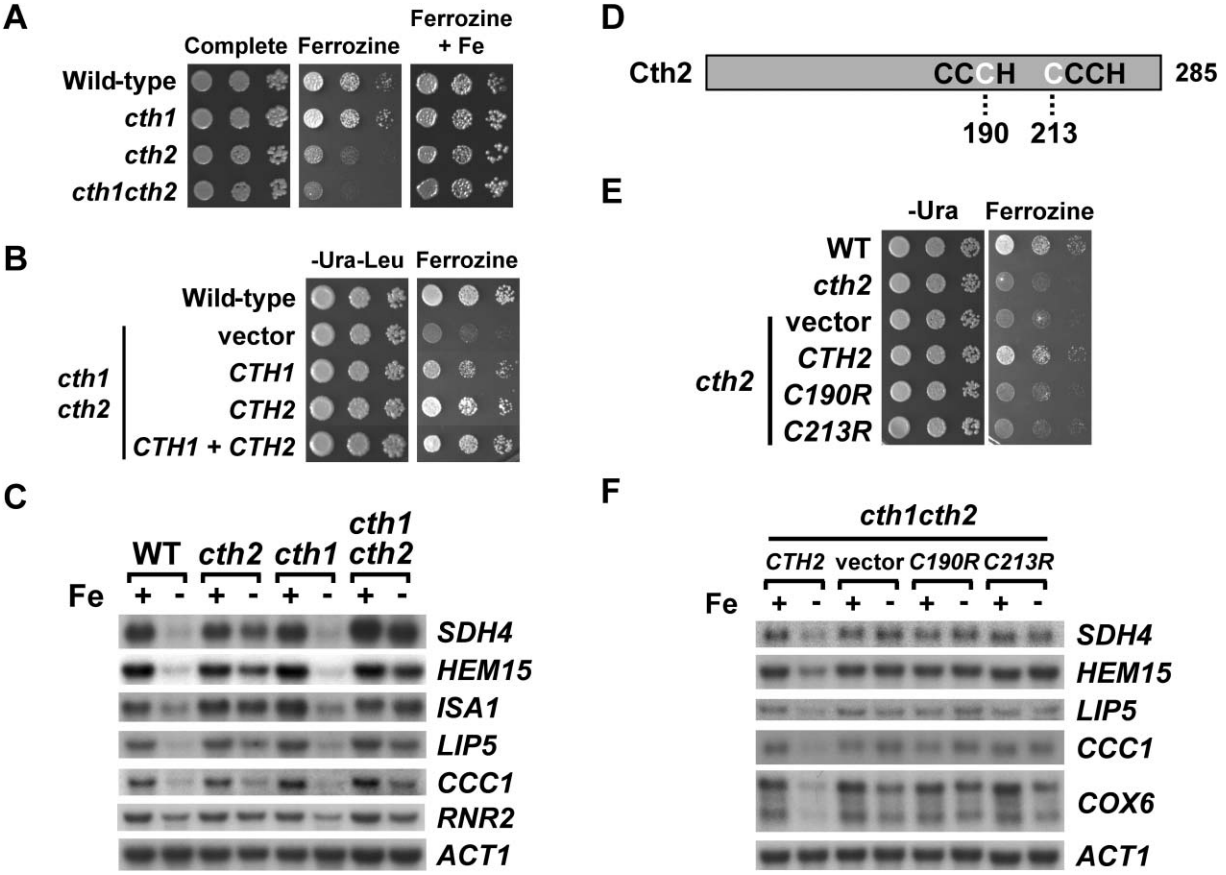

Figure 3. *CTH2* Is Required for Fe-Limited Growth and Fe Deficiency-Dependent mRNA Downregulation

(A) BY4741 wild-type, *cth1*, *cth2*, and *cth1cth2* cells were assayed for growth on SC (Complete) and SC containing 750 μM ferrozine without or with 300 μM Fe (+ Fe).

(B) *cth1cth2* cells cotransformed with pRS416 plus pRS415 (vector), pRS416-CTH1 plus pRS415 (*CTH1*), pRS416 plus pRS415-CTH2 (*CTH2*), and pRS416-CTH1 plus pRS415-CTH2 (*CTH1* + *CTH2*) were assayed on SC-Ura-Leu (−Ura − Leu) and SC containing 750 μM ferrozine.

(C) *CTH2* is essential for Fe deficiency-dependent mRNA downregulation. Wild-type *cth2*, *cth1*, and *cth1cth2* cells were grown in SC media containing 300 μM Fe (Fe +) or 100 μM BPS (Fe −) and RNA extracted and analyzed by RNA blotting.

(D) Schematic representation of the CCCH TZF domain in Cth2 protein. Cysteine residues 190 and 213 (white characters) were mutagenized to arginine.

(E) The Cth2 TZF domains are essential for growth in the presence of ferrozine. BY4741 wild-type and *cth2* cells transformed with vector alone or expressing *CTH2*, *CTH2-C190R*, and *CTH2-C213R* alleles were assayed for growth on ferrozine plates.

(F) The Cth2 CCCH TZF motifs are essential for mRNA downregulation. *cth1cth2* cells containing vector or expressing *CTH2*, *CTH2-C190R*, and *CTH2-C213R* alleles were analyzed by RNA blotting as described for (C).

LIP5, *COX6*, and other mRNAs (data not shown) was abrogated in both Cth2 mutants (Figure 3F). Similar results were obtained when cysteine residues 190 and 213 were mutagenized to alanine (data not shown). Control experiments showed that the cysteine mutant proteins are properly expressed (data not shown). Taken together, these results demonstrate that the integrity of both CCCH zinc finger motifs is essential for Cth2 function in coordinated mRNA downregulation in response to Fe deprivation.

Downregulation of Specific mRNAs by Fe Deprivation Requires AU-Rich Elements

Human TTP binds to AU-rich elements (AREs) within the 3′UTR of target mRNAs and induces RNA degradation (Blackshear et al., 2003; Lai et al., 1999). Interestingly, in silico analysis and visual inspection reveals that approximately 80% of the mRNAs upregulated in *cth2* cells under low Fe conditions contain one or more putative AREs, defined as 5′-UAUUUAUU-3′ and 5′-UUAUU UAU-3′ octamer sequences, located within 500 nucleotides after the translation termination codon (Table 1). To test whether Cth2-dependent mRNA downregulation during Fe deficiency occurs via AREs located within the 3′UTR, we used the mRNA encoding the membrane-anchored heme-containing subunit of the succinate dehydrogenase complex in mitochondria, *SDH4*, which is downregulated under Fe deprivation in a manner completely dependent on Cth2 (Figures 3C and 3F). The *SDH4* 3′UTR contains three 5′-UUAUUUAUU-3′ sequences beginning at 125, 135, and 158 nucleotides after the translation termination codon (Table 1 and Figure 4A). The adenine nucleotides 127, 134, 141, and 160 were mutated to cytosine in a plasmid-borne copy of the *SDH4* gene (Figures 4A and 4B, *SDH4*-AREmt2) and mRNA levels assessed under high and low Fe conditions

Table 1. Genes Upregulated in *cth2* versus Wild-Type Cells under Fe-Limiting Conditions

ORF	Gene	Function	Fold ± SD	Putative AREs
Iron regulon				
YDR534C	FIT1	Cell wall mannoprotein involved in siderophore-Fe uptake	2.0 ± 0.2	263
YOR382W	FIT2	Cell wall mannoprotein involved in siderophore-Fe uptake	1.6 ± 0.1	*255*
YLR205C	HMX1	Heme binding peroxidase involved in reutilization of heme Fe	2.0 ± 0.4	
Heme biosynthesis				
YDR044W	HEM13	Coproporphyrinogen III oxidase, oxygen-requiring enzyme	1.5 ± 0.3[a]	*68, 89*
YOR176W	HEM15	Ferrochelatase, catalyzes insertion of Fe(II) into protoporphyrin IX	2.2 ± 0.2	43, 99
Fe-S cluster biogenesis				
YKL040C	NFU1	NifU-like protein	2.0 ± 0.2	191, 203
YLL027W	ISA1	Member of Fe-S cluster biosynthesis machinery	1.9 ± 0.1	46, 62
TCA cycle				
YNR001C	CIT1	Citrate synthase	2.0 ± 0.2	
YPR001W	CIT3	Mitochondrial isoform of citrate synthase	1.7 ± 0.4	
YLR304C	ACO1	Mitochondrial aconitase, Fe-S cluster protein	2.6 ± 0.3	32, 150, 177
YIL125W	KGD1	Alpha-ketoglutarate dehydrogenase	1.6 ± 0.2	*193, 230*
YDR148C	KGD2	Dihydrolipoyl transsuccinylase	1.8 ± 0.2	242
YLL041C	SDH2	Succinate dehydrogenase (ubiquinone) Fe-S cluster subunit	2.8 ± 0.6	162, *309, 328*
YDR178W	SDH4	Succinate dehydrogenase membrane anchor heme-binding subunit	3.2 ± 0.7	125, 135, 158
YPL262W	FUM1	Mitochondrial and cytoplasmic fumarase, Fe-S cluster protein	1.6 ± 0.2	
Mitochondrial respiration/electron transport chain				
Cytochrome c oxidase				
YGL187C	COX4	Subunit IV of cytochrome c oxidase	1.9 ± 0.4	53
YHR051W	COX6	Subunit VI of cytochrome c oxidase	2.2 ± 0.2	88
YLR395C	COX8	Subunit VIII of cytochrome c oxidase	1.9 ± 0.2	104
YDL067C	COX9	Subunit VIIa of cytochrome c oxidase	1.8 ± 0.2	44
Ubiquinol cytochrome c reductase				
YBL045C	QCR1/COR1	Core subunit I of ubiquinol cytochrome c reductase complex	2.0 ± 0.2	140
YPR191W	QCR2/COR2	Core subunit II of ubiquinol cytochrome c reductase complex	1.6 ± 0.2	155
YFR033C	QCR6/COR3	Subunit VI of ubiquinol cytochrome c reductase complex	1.7 ± 0.3	31
YDR529C	QCR7/COR4	Subunit VII of ubiquinol cytochrome c reductase complex	1.9 ± 0.2	150, *239*
YJL166W	QCR8/COR5	Subunit VIII of ubiquinol cytochrome c reductase complex	1.8 ± 0.3	97, 114
YEL024W	RIP1	Rieske Fe-S protein of ubiquinol cytochrome c reductase complex	2.0 ± 0.1	*293, 355*
YOR356W		Putative mitochondrial dehydrogenase flavoprotein	2.1 ± 0.2	13, 37, 81
YGR255C	COQ6	Flavin-dependent monooxygenase, ubiquinone biosynthesis	1.7 ± 0.3	42
YKR066C	CCP1	Cytochrome c peroxidase	2.8 ± 0.5	18, *41, 50, 59*
YMR145C	NDE1	NADH dehydrogenase	1.6 ± 0.2	
YBL030C	PET9/AAC2	Mitochondrial ADP/ATP carrier	1.6 ± 0.2	
Sterol and fatty acid synthesis and metabolism				
YHR072W	ERG7	Lanosterol synthase	2.0 ± 0.3	*4, 60*
YHR007C	ERG11	Lanosterol C-14 demethylase	1.6 ± 0.1	*174, 203, 273*
YMR208W	ERG12	Mevalonate kinase	1.6 ± 0.1	19
YGR060W	ERG25	C-4 methyl sterol oxidase	1.7 ± 0.4	
YER044C	ERG28	ER membrane protein, may facilitate Erg26 and Erg27 interactions	1.6 ± 0.3	*52*
YGL055W	OLE1	Fatty acid desaturase	1.6 ± 0.3	151, *187*
YMR272C	FAH1/SCS7	Hydroxylation of C-26 fatty acid in ceramide	1.7 ± 0.2	*89, 105*
YPL170W	DAP1	Damage response protein involved in sterol synthesis	1.6 ± 0.1	18, *148*
DNA replication and repair				
YJL026W	RNR2	Ribonucleotide-diphosphate reductase, di-Fe-tyrosyl cofactor	1.4 ± 0.2[a]	68
YGR180C	RNR4	Ribonucleotide-diphosphate reductase, Y4 subunit	1.6 ± 0.4	*39, 125*
Other Fe-, Cu-, and oxygen-related function				
YLR220W	CCC1	Transporter that mediates vacuolar Fe storage	1.4 ± 0.1[a]	*24, 144*
YOR196C	LIP5	Lipoic acid synthase, Fe-S cluster protein	2.0 ± 0.3	70, 92
YGL009C	LEU1	Isopropylmalate isomerase, Fe-S cluster protein	1.7 ± 0.3	85, 123
YDR091C	RLI1	RNase L inhibitor, Fe-S cluster protein	1.6 ± 0.2	*280, 291*
YKL109W	HAP4	Subunit of Hap transcriptional activator	1.7 ± 0.3	*275*, 303
YHR055C	CUP1-2	Copper-binding metallothionein	1.6 ± 0.4	
YAR020C	PAU7	Member of PAU family	1.7 ± 0.2	
YOR394W		Member of PAU family	1.6 ± 0.2	
Other functions				
YCR005C	CIT2	Nonmitochondrial citrate synthase	1.6 ± 0.3	
YDR007W	TRP1	Phosphoribosylanthranilate isomerase	1.8 ± 0.2	*16*
YDR423C	CAD1	Leucine zipper transcriptional activator	1.6 ± 0.3	
YER003C	PMI40	Phosphomannose isomerase	1.6 ± 0.2	54
YHR002W	LEU5	Mitochondrial carrier protein	1.6 ± 0.3	

(*continued*)

Table 1. Continued

ORF	Gene	Function	Fold ± SD	Putative AREs
Other functions				
YJL172W	CPS1	Vacuolar carboxypeptidase	1.7 ± 0.1	
YJR016C	ILV3	Dihydroxyacid dehydratase	1.6 ± 0.2	*98*
YLR121C	YPS3	GPI-anchored aspartic protease	1.7 ± 0.2	*314*
YML028W	TSA1	Thioredoxin-peroxidase	2.0 ± 0.2	
YOR230W	WTM1	WD repeat containing transcriptional modulator I	2.3 ± 0.2	145
YPL053C	KTR6	Mannosylphosphate transferase	1.6 ± 0.2	62
YPL154C	PEP4	Vacuolar proteinase A	1.9 ± 0.3	
Unknown function				
YBL043W	ECM13	Unknown function	1.8 ± 0.1	
YBR187W		Unknown function	1.8 ± 0.1	*109*
YCR017C	CWH43	Putative sensor/transporter protein	1.6 ± 0.3	
YDR366C		Unknown function	1.6 ± 0.2	
YDR411C	DFM1	Der1-like family member	1.8 ± 0.2	
YER048W-A		Unknown function	1.6 ± 0.3	
YER138W-A		Unknown function	1.7 ± 0.3	
YER156C		Unknown function	1.8 ± 0.3	*59*
YGL002W	ERP6	Member of p24 family	1.7 ± 0.1	*71*
YGL188C		Unknown function	1.7 ± 0.1	
YHR045W		Unknown function	1.7 ± 0.2	19
YHR113W		Putative vacuolar aminopeptidase	1.9 ± 0.1	*33*
YJL171C		Unknown function	1.7 ± 0.2	*81*
YKR103W	NFT1	Merged with YKR104 in some backgrounds	3.3 ± 0.4	
YKR104W	NFT1	Putative MRP-type ABC transporter	3.6 ± 0.7	
YLR083C	EMP70	Endosomal membrane protein	1.6 ± 0.2	43, 194
YLR251W	SYM1	Stress-induced yeast MPV17 homologue	1.6 ± 0.2	
YML089C		Unknown function	1.8 ± 0.2	
YMR041C		Unknown function	1.6 ± 0.3	327
YMR110C		Unknown function	1.7 ± 0.3	*83*
YNL320W		Unknown function	1.9 ± 0.2	92
YOL083W		Unknown function	1.8 ± 0.3	*52*
YOL092W		Unknown function	1.8 ± 0.1	*15*
YOR214C		Unknown function	1.6 ± 0.2	
YOR306C	MCH5	Monocarboxylate permease homologue	1.6 ± 0.1	
YPL250C	ICY2	Interacts with the cytoskeleton	1.6 ± 0.1	
YPR002W	PDH1	Homologue to *E. coli* prpD	2.0 ± 0.3	*198*

cth1cth2 cells expressing *CTH2* or vector alone were independently grown by triplicate in the presence of 100 μM BPS (Fe depletion) until exponential cell phase; RNA was extracted, labeled, and hybridized to yeast DNA microarrays as described in Experimental Procedures. The gene expression profile of cells containing vector alone versus expressing *CTH2* (*cth2* versus *CTH2*) was determined and the average fold induction represented. Only mRNAs with a fold induction in the *cth2* mutant higher than 1.6-fold and a p value < 0.05 are shown. ORF, open reading frame systematic name; gene, common name; function, description of the biological function of the protein according to the *Saccharomyces* Genome Database, published data, and sequence homology; AREs, AU-rich elements (5′-UUAUUUAUU-3′ nonamer sequence) positioned within the 500 nucleotides after translation termination codon. 5′-UAUUUAUU-3′ and 5′-UUAUUUAU-3′ octamers were indicated in italics. SD, standard deviation. The complete set of data is available at http://data.cgt.duke.edu/iron.php.

[a] Genes below the cutoff but confirmed by RNA blotting analysis.

by RNA blotting. As shown in Figure 4C, wild-type *SDH4* mRNA levels are dramatically downregulated under Fe depletion, while *SDH4*-AREmt2 mRNA levels are unaffected by Fe. Furthermore, downregulation of *CCC1* mRNA by Fe depletion was also completely dependent on the 3′UTR (Supplemental Figure S3). Taken together, these results demonstrate that *CTH2*-dependent mRNA downregulation under low Fe conditions is dependent on the presence of specific AREs located in the 3′UTR.

To ascertain whether AREs are sufficient for mRNA downregulation in response to Fe deprivation, chimeric transcripts were expressed that contain the coding sequence of *GCN4*, a gene not regulated by Cth2 (data not shown), and the 3′UTR from either *SDH4* or *ACO1* (Figures 4A and 4D), two genes whose mRNA steady-state levels are regulated by Cth2. While wild-type *GCN4* mRNA levels were not significantly decreased by Fe starvation, *GCN4-ACO1-3′UTR* mRNA was dramatically downregulated under Fe deprivation (Figure 4E). A similar result was obtained when the 3′UTR of the *SDH4* mRNA was fused to *GCN4* (Figure 4E). Importantly, mutagenesis of the AREs in the *SDH4-3′UTR* abrogated the Fe dependent downregulation of *GCN4-SDH4-3′UTR* mRNA (Figure 4E, *GCN4-SDH4*-AREmt2). In addition, the downregulation of both *GCN4-ACO1-3′UTR* and *GCN4-SDH4-3′UTR* mRNAs was completely dependent of the presence of a functional Cth2 protein (Figure 4F). *cth1cth2gcn4* mutants expressing either *GCN4-ACO1-3′UTR* or *GCN4-SDH4-3′UTR* were cotransformed with vector, wild-type *CTH2*, or the *CTH2-C190R* mutant. As shown in Figure 4F, the Fe starvation-dependent decrease in steady-state levels for both mRNA species was abrogated in cells lacking *CTH2* (vector lanes) and in cells with a nonfunctional allele of *CTH2*

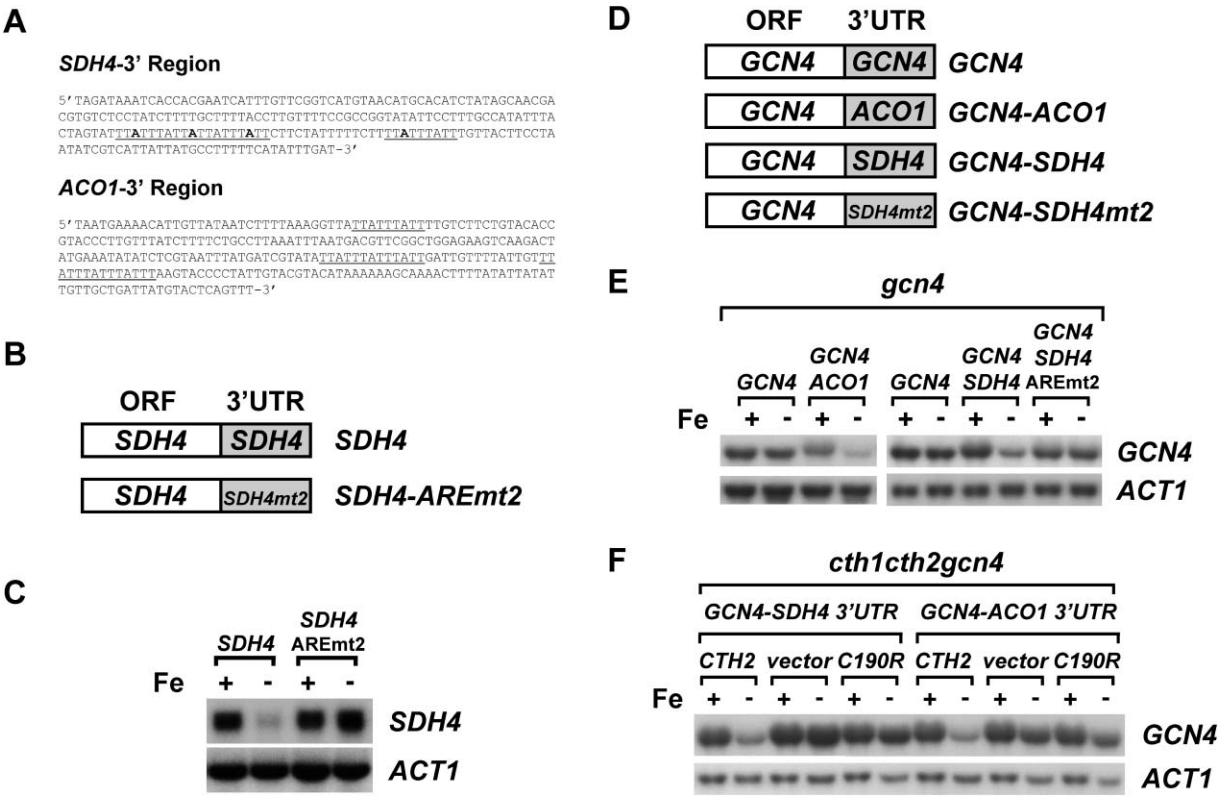

Figure 4. AREs in the 3′UTR of *CTH2* Targets Induce mRNA Destabilization of a Reporter Gene under Fe Scarcity

(A) Sequence of the 3′ region of *SDH4* and *ACO1* genes. Putative AREs are shown underlined. *SDH4-3′UTR* adenine residues mutagenized to cytosine in *GCN4-SDH4-AREmt2* are shown in bold characters.

(B) Schematic representation of wild-type *SDH4* and *SDH4-3′UTR* mutant 2 (*SDH4-AREmt2*).

(C) *SDH4* downregulation in low Fe is dependent on the integrity of the AREs located in the 3′UTR. *sdh4* cells expressing *SDH4* and *SDH4-AREmt2* were grown and analyzed by RNA blotting as described in Figure 3C.

(D) Schematic representation of wild-type *GCN4* and *GCN4* with 3′UTR replaced by *ACO1-3′UTR* (*GCN4-ACO1*), wild-type *SDH4-3′UTR* (*GCN4-SDH4*), and mutant *SDH4*-ARE-*mt2* (*GCN4-SDH4mt2*).

(E) *gcn4* cells expressing *GCN4*, *GCN4-ACO1-3′UTR*, *GCN4-SDH4-3′UTR*, and *GCN4-SDH4-AREmt2* were grown in SC-Ura media (Fe +) and SC-Ura containing 100 μM BPS (Fe −) and analyzed by RNA blotting with *GCN4* and *ACT1* probes.

(F) *cth1cth2gcn4* cells expressing either *GCN4-SDH4-3′UTR* or *GCN4-ACO1-3′UTR* were transformed with vector alone or containing *CTH2* or *CTH2-C190R* mutant allele and grown and analyzed by RNA blotting as described (E).

(*C190R* lanes). Taken together, these results demonstrate that the AREs found in the 3′UTR of both *ACO1* and *SDH4* are necessary and sufficient to induce the *CTH2* and Fe limitation-dependent downregulation of *GCN4* mRNA.

Cth2 Accelerates the Rate of mRNA Decay

Our data strongly implicate Cth2 and 3′UTR AREs in the coordinated downregulation of specific mRNAs by Fe deprivation. Steady-state mRNA measurements are the net consequence of both transcription and the rate of mRNA decay, and our analyses are consistent with Cth2 acting at a posttranscriptional level. To evaluate the effects of Cth2 on mRNA decay rates, two Cth2-dependent target mRNAs were conditionally expressed in yeast using the galactose-inducible and glucose-repressible *GAL1* promoter. *cth1cth2gcn4* cells were cotransformed with *GCN4-ACO1-3′UTR* or *GCN4-SDH4-3′UTR* constructs driven by the *GAL1* promoter (Figure 5) and plasmid-borne *CTH2* or empty vector. Cells were grown in galactose and the Fe chelator BPS to induce transcription of *GCN4-ACO1/SDH4-3′UTR* and *CTH2*, respectively. Transcription of the *GCN4-ACO1* or *GCN4-SDH4-3′UTR* genes was shut off by glucose addition and mRNA levels analyzed over time by RNA blotting (Figure 5). The half-life of *GCN4-ACO1-3′UTR* mRNA decreased from 7 min to 3 min when *CTH2* was expressed (Figure 5A). A similar decrease in the half-life, from 9 to 4 min, was observed for *GCN4-SDH4-3′UTR* mRNA in cells expressing *CTH2* (Figure 5B). No change in mRNA half-life was observed when the cells expressed the *CTH2-C190R* mutant allele or when they were grown in the presence of Fe, conditions that severely repress the expression of *CTH2* (data not shown). Furthermore, while the half-life of a mRNA including the *SDH4* coding sequence and 3′UTR was 7 min in wild-type cells growing under Fe-deficient conditions, it increased to 14 min in either cells lacking *CTH2*, wild-type cells grown in Fe-replete conditions, or in *CTH2* wild-type cells expressing *SDH4* mRNA with mutated AREs (Figure 5C). Similar results were obtained for the

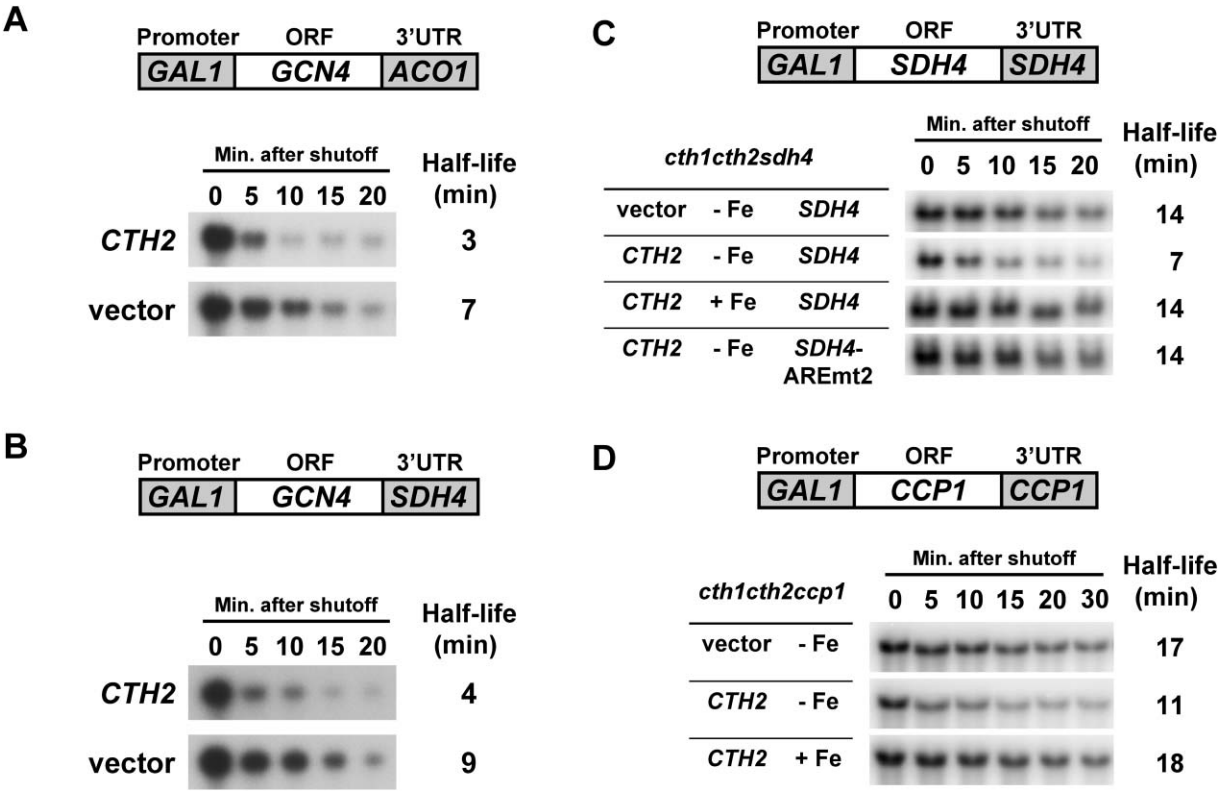

Figure 5. Cth2 Accelerates the Decay of mRNAs Containing *ACO1*, *SDH4, or CCP1* 3′UTRs

cth1cth2gcn4 cells containing either p415GAL1-GCN4-ACO1-3′UTR (A) or p415GAL1-GCN4-SDH4-3′UTR (B) plasmids were cotransformed with pRS416-CTH2 (*CTH2*) and pRS416 (vector). Cells were grown in galactose under low Fe (and Fe replete, data not shown) conditions until exponential growth phase. Then glucose was added to stop transcription of *GCN4-ACO1* and *GCN4-SDH4* mRNAs and total RNA extracted and analyzed by RNA blotting. (C) *cth1cth2sdh4* cells containing either p415GAL1-SDH4 or p415GAL1-SDH4-AREmt2 plasmids were cotransformed with pRS416-CTH2 (*CTH2*) and pRS416 (vector). (D) *cth1cth2ccp1* cells containing plasmid p415GAL1-CCP1 were cotransformed with pRS416-CTH2 (*CTH2*) and pRS416 (vector). Cells were grown and treated as described for (A) and (B). *GCN4*, *SDH4*, and *CCP1* mRNA values were normalized with *ACT1* loading control. mRNA half-lives were calculated on the basis of at least two independent experiments.

half-life measurements of the cytochrome c peroxidase *CCP1* mRNA (Figure 5D). Taken together, these results demonstrate that *CTH2* accelerates the destabilization of mRNAs containing *ACO1*, *SDH4*, or *CCP1* 3′UTRs, which harbor AREs that function through Cth2.

Cth2 Binds to *SDH4* and *ACO1* AU-Rich Elements

To understand how Cth2 coordinately stimulates the decay of a large battery of specific mRNA molecules in response to Fe deprivation in a 3′UTR-dependent manner, we ascertained whether Cth2 binds to AREs in vivo using the yeast three-hybrid system (Putz et al., 1996; SenGupta et al., 1996). Sequences from both the *ACO1* and *SDH4* 3′UTRs containing functional AREs were fused to bacteriophage MS2 RNA and coexpressed in yeast cells expressing a Cth2-Gal4 *trans*-activation domain fusion protein (Figures 6A and 6B). Cells coexpressing either the *ACO1* or *SDH4* 3′UTR fusion RNAs, together with wild-type *CTH2*, grow in medium lacking histidine, indicative of an interaction between Cth2 and the 3′UTR of each mRNA (Figure 6C). Moreover, consistent with our evidence that Cth2 cysteine residue 190 (as well as cysteine 213) is required to mediate target mRNA destabilization in vivo, this interaction is severely compromised when the *ACO1* or *SDH4* ARE-MS2 RNA is coexpressed with the Cth2 C190R-Gal4 activation domain fusion, which is expressed at levels similar to Cth2-Gal4 fusion protein (Figure 6C, data not shown).

To further test the specificity of this Cth2-ARE interaction, we mutagenized the AREs contained in the *SDH4*-MS2 fusion RNA. As shown in Figure 6C, mutagenesis of adenine nucleotides 127, 134, and 141 to cytosine (Figure 6B, mt1) decreased growth on minus histidine plates, while the additional substitution of adenine nucleotide 160 to cytosine (Figure 6B, mt2) completely abrogated growth, suggesting that Cth2 binding to the *SDH4-3′UTR* mRNA occurs through two ARE regions. Additional evidence for differential binding between Cth2 and the two mutant ARE alleles is evident from both the addition of the His3 inhibitor 3-aminotriazole (Figure 6C) and β-galactosidase assays demonstrating that Cth2 interaction with the *SDH4* 3′UTR is reduced to one third in *SDH4*-mt1 and almost completely abrogated when all *SDH4* AREs are mutated (Figure 6D, *SDH4*-mt2). These results strongly suggest that Cth2 binds target mRNAs in vivo in a manner that is dependent upon the functional integrity of both the CCCH tandem

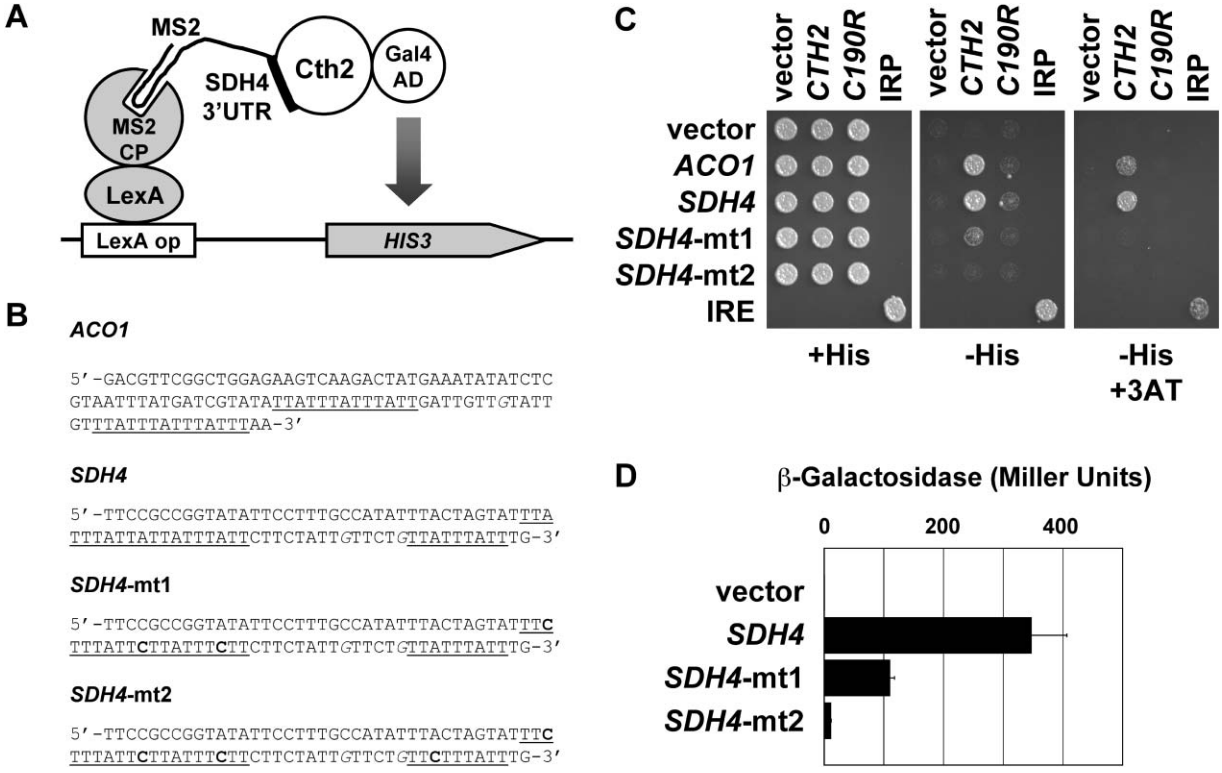

Figure 6. Cth2 Protein Specifically Interacts with AREs within *ACO1* and *SDH4* mRNAs

(A) Schematic representation of the yeast three-hybrid strategy (SenGupta et al., 1996) applied to monitor the in vivo interaction between Cth2 protein and 3′UTR-RNA.

(B) 3′UTR sequences used in the yeast three-hybrid assay. The MS2 RNA was fused to *ACO1*, *SDH4* wild-type, and *SDH4* mutant 3′UTR sequences. *SDH4-3′UTR* sequence was mutagenized in one (mt1) or both ARE patches (mt2) shown as underlined. Gs in italics substituted Us to avoid premature termination of the RNA polymerase III transcription.

(C) Cells expressing wild-type Cth2 and 3′UTR from *ACO1* and wild-type *SDH4* grow in the absence of histidine. L40-coat cells were cotransformed with (1) pIIIA/MS2-1 vector alone and containing the 3′UTR from *ACO1*, *SDH4*, *SDH4*-mt1, *SDH4*-mt2, and the iron-response element (IRE) as a positive control; and (2) pACT2 vector alone and fused to *CTH2*, *CTH2-C190R*, and the iron-responsive protein (IRP) as a positive control. Cells were grown on SC-Leu-Ura (+His), SC-Leu-Ura-His (−His), and SC-Leu-Ura-His + 1 mM 3-aminotriazol (−His + 3AT). The same result was obtained with fusions to pIIIA/MS2-2 vector (data not shown).

(D) Cth2 interaction with *SDH4-3′UTR* depends on the integrity of *SDH4* AREs. L40-coat cells cotransformed with (1) pACT2-CTH2 and (2) pIIIA/MS2-1 fused to the 3′UTR from *SDH4*, *SDH4*-mt1, and *SDH4*-mt2 were grown on SC-Leu-Ura and assayed for β-galactosidase activity in six independent experiments.

zinc finger motifs and specific AU-rich elements in the 3′UTR of the mRNAs that exhibit decreased steady-state levels in response to Fe deprivation.

Discussion

While our understanding of Fe uptake and distribution mechanisms has advanced greatly in recent years, the metabolic reprogramming of cells in response to Fe deprivation and the mechanisms that underlie these events are not well understood. We have addressed this question using the eukaryotic microorganism *S. cerevisiae*, for which the mechanisms involved in Fe sensing, Fe uptake, and distribution are well understood. Studies on these genes and their functional orthologs in humans have led to important insights into Fe homeostasis and diseases of Fe imbalance (Hentze et al., 2004; Nittis and Gitlin, 2002; Roy and Andrews, 2001). By using DNA microarrays, we have discovered that multiple components of Fe-dependent pathways are downregulated at the mRNA level in response to Fe depletion. While genome-wide expression profiles of yeast cells grown under Fe limitation have been reported (Shakoury-Elizeh et al., 2004), most of the Fe-regulated genes identified here have not been previously reported due to the use of mild Fe deprivation conditions. Importantly, we have characterized the molecular mechanism that governs this global coordinated response to Fe deficiency. We demonstrate that Cth2, which is specifically induced under Fe deprivation, binds to AREs within the 3′UTR of specific mRNAs and accelerates their degradation.

Our DNA microarray data indicate that Cth2 downregulates the steady-state levels of mRNAs coding for proteins that participate in multiple Fe-dependent metabolic pathways including the TCA cycle, respiration, lipid metabolism, heme biosynthesis, and multiple Fe-S proteins, as well as many proteins of as yet unknown function. The majority of these mRNAs contain one or more

5′-UUAUUUAUU-3′ nonamers within the 3′UTR, strongly suggesting that they may be direct targets for Cth2-mediated degradation. Interestingly, genes highly affected by Cth2 defects, such as *HEM15*, *ACO1*, *SDH2*, and *SDH4*, contain two or more overlapping 5′-UUAUU-UAUU-3′ nonamers, while other genes more modestly affected, such as the essential subunit of the Fe-dependent enzyme ribonucleotide reductase encoded by *RNR2*, only contain a single 5′-UUAUUUAU-3′ octamer (Table 1). However, one third of the genes affected in a *cth2* mutant strain do not contain AU-rich sequences defined as 5′-UUAUUUAU-3′ or 5′-UAUUUAUU-3′ octamer sequences within 500 nucleotides downstream of the translation termination codon. A recent report has shown that, although the optimal RNA binding motif for the CCCH tandem zinc fingers of TTP is the 5′-UUAUUUAUU-3′ nonamer, other U-rich sequences containing the motif AU_nA (n = 2–5) may serve as moderate high-affinity binding sites (Brewer et al., 2004). Therefore, a possible explanation for our microarray results is that ARE variants from the 5′-UUAUUUAU-3′ or 5′-UAUUUAUU-3′ octamer sequences may also modulate Cth2-dependent regulation. It is also possible that changes in these mRNAs are a consequence of an indirect effect of the *cth2* mutation and, therefore, misregulated Fe homeostasis. In this sense, several genes including the other two subunits of the ribonucleotide reductase complex *RNR1* and *RNR3*, stress-response genes such as *HSP12* and *SSA1*, and genes located near telomeres are significantly downregulated in *cth2* mutants (data not shown). Therefore, the genome-wide studies in *cth2* cells under Fe deficiency may provide important information about both primary and secondary responses of cells to misregulation in Fe-dependent pathways.

Biosynthesis of sterol and unsaturated fatty acids are essential processes that depend on both oxygen and Fe. It has been previously shown that these genes are specifically induced under hypoxic conditions, perhaps in an attempted compensatory response to reduced oxygen tension (Kwast et al., 2002). Interestingly, in this study, we show that the mRNA levels of genes involved in sterol synthesis (*ERG* genes) and unsaturated fatty acid biosynthesis (*OLE1*) increase upon Fe depletion. A potential explanation for this observation is that the activity of Fe-requiring proteins in these pathways is reduced, thereby limiting the levels of reaction products and resulting in decreased feedback inhibition and increased gene transcription. In addition, we also demonstrate that the steady-state levels of *ERG* and *OLE1* mRNAs are elevated in *cth2* cells, suggesting that Cth2 protein plays a role in the destabilization of these mRNAs (Table 1 and data not shown). Furthermore, steady-state levels of mRNAs expressed from two members of the Fe regulon, *FIT1* and *FIT2*, are also upregulated in response to Fe depletion via Aft1-Aft2 and downregulated in the presence of a functional Cth2. The presence of multiple putative AREs in the 3′UTR of these genes strongly suggests that they are direct targets for Cth2 regulation. We propose that this opposite transcriptional and posttranscriptional control of mRNA levels provides cells with an additional degree of flexibility that optimizes its response to changing Fe availability by rapidly affecting transcript abundance through alterations in transcriptional rates and mRNA stability.

Both our genome-wide transcript analyses and the growth defect of *cth2* mutants under Fe-limiting conditions suggest that yeast cells undergo a Cth2-mediated global metabolic reprogramming in response to Fe deficiency to facilitate the utilization of limited available Fe levels. In response to Fe limitation, bacteria utilize the ferric uptake repressor protein Fur for transcriptional derepression of many genes directly or indirectly involved in Fe acquisition (McHugh et al., 2003). Fur also induces the expression of small RNAs, RyhB in *Escherichia coli* and PrrF1 and Prrf2 in *Pseudomonas aeruginosa*. Interestingly, these antisense RNAs stimulate the degradation of mRNAs coding for the Fe-S cluster-containing enzymes of the TCA cycle, Fe storage proteins, and an Fe-dependent superoxide dismutase (Masse and Gottesman, 2002; Wilderman et al., 2004). But why do cells downregulate Fe-dependent pathways posttranscriptionally? The relative contribution of mRNA decay to steady-state mRNA levels and gene expression is often underestimated. Recent studies show that approximately 50% of changes in transcript levels occurring in response to environmental changes are associated with mRNA turnover (Fan et al., 2002; Khodursky and Bernstein, 2003). Furthermore, coordinated regulation of functionally related mRNAs at the level of transcript stability is known in both prokaryotic and eukaryotic cells and has been proposed to represent the posttranscriptional functional equivalent of a bacterial operon or decay operon (Gerber et al., 2004; Keene and Tenenbaum, 2002; Tenenbaum et al., 2000; Wilusz et al., 2001).

Mammalian cells express three proteins that contain two $Cx_8Cx_5Cx_3H$ TZF domains: TTP, CMG1, and TIS11D (Blackshear, 2002). The best-characterized member of this family is human tristetraprolin (Blackshear, 2002; Carballo et al., 1998; Sawaoka et al., 2003; Stoecklin et al., 2001). The other two TTP-family members can also destabilize ARE-containing mRNAs but are regulated and expressed differently (Blackshear, 2002). These results, and the observation that yeast cells indeed regulate mRNA decay via AREs (Vasudevan and Peltz, 2001), raise the question of whether the mammalian TTP isoforms function in Fe homeostasis. Furthermore, our experiments suggest that the Cth2 homolog Cth1, while not Fe regulated, may also contribute to a small extent to Fe homeostasis (data not shown); however, other Cth1 cellular functions are also possible. Interestingly, we have recently identified the *CTH1* promoter as a target for the heat shock transcription factor HSF (Hahn et al., 2004). Here we describe a master regulatory mechanism that dictates the response of eukaryotic cells to Fe deficiency. A single regulatory protein, Cth2, controls the coordinated response of multiple Fe-dependent metabolic pathways to Fe deficiency by targeting specific mRNA molecules for degradation. This mechanism of regulation represents a functional "posttranscriptional Fe regulon" that optimizes the utilization of limited available Fe.

Experimental Procedures

Yeast Strains and Growth Conditions

Genotypes for the yeast strains used in this study are listed in Supplemental Table S1. To test growth under conditions of Fe depri-

vation, cells were grown in synthetic media (SC) or SC lacking specific requirements (SC minus) to exponential phase (A_{600} = 1.0), spotted in 10-fold serial dilutions starting at A_{600}= 0.1 on SC + 750 μM ferrozine, and incubated at 30°C for 4–7 days.

Plasmids

CTH1, *CTH2*, and *CCC1* sequences were cloned into pRS416 and pRS415 vectors. Two copies of the Flag epitope were introduced after the *CTH2* start codon to generate a Flag-tagged Cth2 allele. *CTH2-C190R* and *CTH2-C213R* were PCR amplified using the overlap extension method (Puig et al., 2002) and cloned into pRS416 and pRS415 vectors. The *CCC1* sequence was cloned into pRS416 containing the *CYC1* terminator. We used the overlap extension method to mutagenize the Aft1 consensus binding sites in the *CTH2* upstream sequence. Plasmids containing *AFT1-1^{up}* or *AFT2-1^{up}* mutant alleles were a generous gift from Dr. D. Winge (University of Utah). The *GCN4* sequence was cloned into pRS416. *GCN4* sequence with no 3′UTR (pRS416-GCN4-No-3′UTR) was cloned into pRS416 and p415GAL1. The *ACO1* and *SDH4* 3′UTRs were cloned into pRS416-GCN4-No-3′UTR. The *SDH4* and *CCP1* coding and 3′UTR sequences were cloned into pRS416 and p415GAL1 vectors. Both *GCN4-SDH4-AREmt2* and *SDH4-AREmt2* were generated by the overlap extension method. *ACO1*, *SDH4*, *SDH4-AREmt1*, and *SDH4-AREmt2* 3′UTR sequences were cloned into SmaI-digested pIIIA/MS2-1 and pIIIA/MS2-2, a gift from Dr. Marvin Wickens (University of Wisconsin). Wild-type *CTH2* and *CTH2-C190R* allele were cloned in fusion to Gal4 activation domain in pACT2 vector. All PCR amplifications were performed with *Pfu* Turbo DNA polymerase (Stratagene), and inserts were sequenced.

RNA Blot Analysis

Cells were grown in SC, or SC lacking specific requirements (SC minus), containing 100–300 μM $Fe(NH_4)_2(SO_4)_2$ (Fe +) or 100 μM BPS (Fe −) to exponential phase. Total yeast RNA was isolated with a modified hot phenol method (Puig et al., 2002). PCR-amplified fragments were gel purified and radiolabeled with ^{32}P-dCTP to be used as probes. Actin (*ACT1*) was used as a loading control.

DNA Microarrays

Wild-type BY4741, *cth2*, and *cth1cth2* mutant cells for microarray experiments were grown in SC containing 300 μM $Fe(NH_4)_2(SO_4)_2$ (Fe +) or 100 μM BPS (Fe −) to exponential phase. RNA was isolated and processed as previously described (Puig et al., 2004). Experiments were independently performed in triplicate, and a p value $<$ 0.05 was used. For further information about preparation of the slides for microarrays, synthesis of fluorescent-labeled cDNA, hybridization, scanning and data acquisition, and quality control steps, visit the Duke Microarray Core Facility at http://mgm.duke.edu/genome/dna_micro/core. Data were analyzed using GeneSpring 6.1 (Silicon Genetics).

mRNA Decay Experiments

Cells were grown overnight in SC-raffinose-Ura-Leu (2% raffinose–no glucose) and reinoculated in SC-galactose-Ura-Leu (2% raffinose–4% galactose) with 100 μM BPS until exponential growth phase. Glucose was added to a final concentration of 4% to terminate transcription of *GCN4* chimeric mRNAs and aliquots taken at 5, 10, 15, and 20 min time points. Total RNA was extracted, analyzed by RNA blotting with *GCN4* and *ACT1* probes, and quantitated with a STORM 840 phosphoimager (Amersham Biosciences). *GCN4* values were normalized with *ACT1* values. The half-life was calculated as the average of three independent experiments.

Yeast Three-Hybrid Assays

β-galactosidase, protein extraction and analysis by immunoblot, and yeast three-hybrid assays were performed as previously described (Puig et al., 2002; SenGupta et al., 1996).

Acknowledgments

We are grateful to the members of the Thiele laboratory for helpful suggestions and to Drs. Perry Blackshear, Wi Lai, Jack Keene, Ji-Sook Hahn, and Dan Neef for comments on the manuscript. We also thank Jordan Cocchiaro, Xiao-Hong Jiang, Chen Kuang, and Miranda Lau for excellent technical assistance; Drs. D. Winge, C. Moehle, P. Blackshear, P. Blaiseau, M. Wickens, and D. Kuhl for generously providing yeast strains and plasmids used in this study; and Dr. Holly Dressman from the Duke Microarray Core Facility. This work was supported by grant GM41840 from the National Institutes of Health to D.J.T.

Received: July 19, 2004
Revised: October 19, 2004
Accepted: November 9, 2004
Published: January 13, 2005

References

Baynes, R.D., and Bothwell, T.H. (1990). Iron deficiency. Annu. Rev. Nutr. *10*, 133–148.

Blackshear, P.J. (2002). Tristetraprolin and other CCCH tandem zinc-finger proteins in the regulation of mRNA turnover. Biochem. Soc. Trans. *30*, 945–952.

Blackshear, P.J., Lai, W.S., Kennington, E.A., Brewer, G., Wilson, G.M., Guan, X., and Zhou, P. (2003). Characteristics of the interaction of a synthetic human tristetraprolin tandem zinc finger peptide with AU-rich element-containing RNA substrates. J. Biol. Chem. *278*, 19947–19955.

Blaiseau, P.L., Lesuisse, E., and Camadro, J.M. (2001). Aft2p, a novel iron-regulated transcription activator that modulates, with Aft1p, intracellular iron use and resistance to oxidative stress in yeast. J. Biol. Chem. *276*, 34221–34226.

Brewer, B.Y., Malicka, J., Blackshear, P.J., and Wilson, G.M. (2004). RNA sequence elements required for high affinity binding by the zinc finger domain of tristetraprolin: conformational changes coupled to the bipartite nature of Au-rich MRNA-destabilizing motifs. J. Biol. Chem. *279*, 27870–27877.

Carballo, E., Lai, W.S., and Blackshear, P.J. (1998). Feedback inhibition of macrophage tumor necrosis factor-alpha production by tristetraprolin. Science *281*, 1001–1005.

Escolar, L., Perez-Martin, J., and de Lorenzo, V. (1999). Opening the iron box: transcriptional metalloregulation by the Fur protein. J. Bacteriol. *181*, 6223–6229.

Fan, J., Yang, X., Wang, W., Wood, W.H., III, Becker, K.G., and Gorospe, M. (2002). Global analysis of stress-regulated mRNA turnover by using cDNA arrays. Proc. Natl. Acad. Sci. USA *99*, 10611–10616.

Foury, F., and Talibi, D. (2001). Mitochondrial control of iron homeostasis. A genome wide analysis of gene expression in a yeast frataxin-deficient strain. J. Biol. Chem. *276*, 7762–7768.

Gerber, A.P., Herschlag, D., and Brown, P.O. (2004). Extensive association of functionally and cytotopically related mRNAs with Puf family RNA-binding proteins in yeast. PLoS Biol 2(3): e79 DOI: 10.1371/journal.pbio.0020079

Hahn, J.S., Hu, Z., Thiele, D.J., and Iyer, V.R. (2004). Genome-wide analysis of the biology of stress responses through heat shock transcription factor. Mol. Cell. Biol. *24*, 5249–5256.

Hentze, M.W., Muckenthaler, M.U., and Andrews, N.C. (2004). Balancing acts: molecular control of mammalian iron metabolism. Cell *117*, 285–297.

Keene, J.D., and Tenenbaum, S.A. (2002). Eukaryotic mRNPs may represent posttranscriptional operons. Mol. Cell *9*, 1161–1167.

Khodursky, A.B., and Bernstein, J.A. (2003). Life after transcription—revisiting the fate of messenger RNA. Trends Genet. *19*, 113–115.

Kwast, K.E., Lai, L.C., Menda, N., James, D.T., III, Aref, S., and Burke, P.V. (2002). Genomic analyses of anaerobically induced genes in *Saccharomyces cerevisiae*: functional roles of Rox1 and other factors in mediating the anoxic response. J. Bacteriol. *184*, 250–265.

Lai, W.S., Carballo, E., Strum, J.R., Kennington, E.A., Phillips, R.S., and Blackshear, P.J. (1999). Evidence that tristetraprolin binds to AU-rich elements and promotes the deadenylation and destabilization of tumor necrosis factor alpha mRNA. Mol. Cell. Biol. *19*, 4311–4323.

Lai, W.S., Kennington, E.A., and Blackshear, P.J. (2003). Tristetraprolin and its family members can promote the cell-free deadenylation of AU-rich element-containing mRNAs by poly(A) ribonuclease. Mol. Cell. Biol. *23*, 3798–3812.

Lesuisse, E., Santos, R., Matzanke, B.F., Knight, S.A., Camadro, J.M., and Dancis, A. (2003). Iron use for haeme synthesis is under control of the yeast frataxin homologue (Yfh1). Hum. Mol. Genet. *12*, 879–889.

Masse, E., and Gottesman, S. (2002). A small RNA regulates the expression of genes involved in iron metabolism in *Escherichia coli*. Proc. Natl. Acad. Sci. USA *99*, 4620–4625.

McHugh, J.P., Rodriguez-Quinones, F., Abdul-Tehrani, H., Svistunenko, D.A., Poole, R.K., Cooper, C.E., and Andrews, S.C. (2003). Global iron-dependent gene regulation in *Escherichia coli*. A new mechanism for iron homeostasis. J. Biol. Chem. *278*, 29478–29486.

Nittis, T., and Gitlin, J.D. (2002). The copper-iron connection: hereditary aceruloplasminemia. Semin. Hematol. *39*, 282–289.

Puig, S., Lee, J., Lau, M., and Thiele, D.J. (2002). Biochemical and genetic analyses of yeast and human high affinity copper transporters suggest a conserved mechanism for copper uptake. J. Biol. Chem. *277*, 26021–26030.

Puig, S., Lau, M., and Thiele, D.J. (2004). Cti6 is an Rpd3-Sin3 histone deacetylase-associated protein required for growth under iron-limiting conditions in *Saccharomyces cerevisiae*. J. Biol. Chem. *279*, 30298–30306.

Putz, U., Skehel, P., and Kuhl, D. (1996). A tri-hybrid system for the analysis and detection of RNA-protein interactions. Nucleic Acids Res. *24*, 4838–4840.

Roy, C.N., and Andrews, N.C. (2001). Recent advances in disorders of iron metabolism: mutations, mechanisms and modifiers. Hum. Mol. Genet. *10*, 2181–2186.

Rutherford, J.C., Jaron, S., and Winge, D.R. (2003). Aft1p and Aft2p mediate iron-responsive gene expression in yeast through related promoter elements. J. Biol. Chem. *278*, 27636–27643.

Sawaoka, H., Dixon, D.A., Oates, J.A., and Boutaud, O. (2003). Tristetraprolin binds to the 3′-untranslated region of cyclooxygenase-2 mRNA. A polyadenylation variant in a cancer cell line lacks the binding site. J. Biol. Chem. *278*, 13928–13935.

SenGupta, D.J., Zhang, B., Kraemer, B., Pochart, P., Fields, S., and Wickens, M. (1996). A three-hybrid system to detect RNA-protein interactions in vivo. Proc. Natl. Acad. Sci. USA *93*, 8496–8501.

Shakoury-Elizeh, M., Tiedeman, J., Rashford, J., Ferea, T., Demeter, J., Garcia, E., Rolfes, R., Brown, P.O., Botstein, D., and Philpott, C.C. (2004). Transcriptional remodeling in response to iron deprivation in *Saccharomyces cerevisiae*. Mol. Biol. Cell *15*, 1233–1243.

Stoecklin, G., Stoeckle, P., Lu, M., Muehlemann, O., and Moroni, C. (2001). Cellular mutants define a common mRNA degradation pathway targeting cytokine AU-rich elements. RNA *7*, 1578–1588.

Tenenbaum, S.A., Carson, C.C., Lager, P.J., and Keene, J.D. (2000). Identifying mRNA subsets in messenger ribonucleoprotein complexes by using cDNA arrays. Proc. Natl. Acad. Sci. USA *97*, 14085–14090.

Theil, E.C. (2000). Targeting mRNA to regulate iron and oxygen metabolism. Biochem. Pharmacol. *59*, 87–93.

Thompson, M.J., Lai, W.S., Taylor, G.A., and Blackshear, P.J. (1996). Cloning and characterization of two yeast genes encoding members of the CCCH class of zinc finger proteins: zinc finger-mediated impairment of cell growth. Gene *174*, 225–233.

Van Ho, A., Ward, D.M., and Kaplan, J. (2002). Transition metal transport in yeast. Annu. Rev. Microbiol. *56*, 237–261.

Vasudevan, S., and Peltz, S.W. (2001). Regulated ARE-mediated mRNA decay in *Saccharomyces cerevisiae*. Mol. Cell *7*, 1191–1200.

Wilderman, P.J., Sowa, N.A., FitzGerald, D.J., FitzGerald, P.C., Gottesman, S., Ochsner, U.A., and Vasil, M.L. (2004). Identification of tandem duplicate regulatory small RNAs in *Pseudomonas aeruginosa* involved in iron homeostasis. Proc. Natl. Acad. Sci. USA *101*, 9792–9797.

Wilusz, C.J., Wormington, M., and Peltz, S.W. (2001). The cap-to-tail guide to mRNA turnover. Nat. Rev. Mol. Cell Biol. *2*, 237–246.

Yamaguchi-Iwai, Y., Stearman, R., Dancis, A., and Klausner, R.D. (1996). Iron-regulated DNA binding by the AFT1 protein controls the iron regulon in yeast. EMBO J. *15*, 3377–3384.